JOURNAL OF PROPULSION AND POWER
Vol. 16, No. 4, July–August 2000

Transition in Boundary Layers on a Concave Surface

S. H. Winoto,* D. H. Zhang,† and Y. T. Chew‡
National University of Singapore, Singapore 119260, Republic of Singapore

Transition from laminar to turbulent flow has been investigated in boundary layers along a concave surface of 2.0 m radius of curvature for a freestream velocity range of 6.0–15.0 m/s. Velocity and turbulent intermittency measurements were made using a single sensor hot-wire anemometer. Intermittency profiles at the so-called upwash and downwash regions were obtained at some streamwise positions to help determine the transition starts and ends at the regions. The experimental results show that, at both upwash and downwash regions for all of the free-stream velocities tested, the intermittency profiles at different transition stages exhibit similar behaviors. The difference between the upwash and downwash intermittency profiles obtained at the same streamwise locations decreases with increasing freestream velocity. For all of the freestream velocities, transition starts and ends earlier at the upwash regions than at the downwash regions. The transition lengths in the upwash regions are slightly longer than those in the downwash regions and decrease with increasing freestream velocity. The starts of transition at the upwash regions agree well with the transition prediction Goertler number of 6, whereas at the ends of transition for both upwash and downwash regions, the Goertler number ranges from 7.90 to 9.30.

Nomenclature

C = threshold constant
C_p = static pressure coefficient, $(p - p_R)/0.5\rho U_R^2$
G_θ = Goertler number, $(U_0\theta/\nu)(\theta/R)^{1/2}$
p = static pressure
p_R = reference static pressure measured where x is 200 mm
R = radius of concave surface
Re_θ = Reynolds number based on boundary-layer momentum thickness, $U_0\theta/\nu$
Tu = freestream turbulence intensity
t = time
U_R = reference freestream velocity where x is 200 mm
U_0 = freestream velocity
$\bar{u}$ = streamwise mean velocity
u' = streamwise fluctuating velocity
x = streamwise direction or distance measured from concave surface leading edge
$x_{tr,e}$ = streamwise transition end position
$x_{tr,s}$ = streamwise transition start position
y = normal direction or distance to concave surface
z = spanwise direction or distance measured from centre-line of concave surface
α = wave number
β = vortex amplification factor
γ = turbulent intermittency factor
δ = boundary-layer thickness
δ^* = boundary-layer displacement thickness
η = nondimensional parameter, $y/(x\nu/U_0)^{1/2}$
θ = boundary-layer momentum thickness
Λ = nondimensional wavelength parameter, $(U_0R/\nu)(\lambda/R)^{3/2}$
λ = wavelength of Goertler vortices
ν = fluid kinematic viscosity
ξ = nondimensional parameter, $(x - x_{tr,s})/(x_{tr,e} - x_{tr,s})$
ρ = fluid density

Received 3 December 1998; revision received 12 February 2000; accepted for publication 16 March 2000.

*Associate Professor, Department of Mechanical and Production Engineering, 10 Kent Ridge Crescent.
†Research Scholar, Department of Mechanical and Production Engineering, 10 Kent Ridge Crescent.
‡Professor, Department of Mechanical and Production Engineering, 10 Kent Ridge Crescent.

I. Introduction

TRANSITION in a boundary-layer flow on a solid body is affected by many parameters, such as the pressure distribution in the freestream flow, the surface roughness, and the freestream turbulence level.[1,2] Knowledge of transition in a boundary-layer flow on a solid body surface is very important if calculations of boundary-layer development (which may include drag and heat transfer) are to be reliable. Also, the boundary-layer parameters, such as skin friction and heat transfer coefficient, are known to undergo continuous but significant change through the transition region.

The process of transition in the boundary layer on a flat plate at zero incidence is somewhat simpler than that on a concave surface with streamwise curvature. This is because the laminar boundary layer developed along the concave surface will be subjected to centrifugal instability that manifests itself as a system of streamwise counter-rotating vortices (Fig. 1) named after Goertler,[3] who first predicted their occurrence analytically. These vortices distribute streamwise momentum, which results in periodic spanwise variations of streamwise velocity component $\bar{u}$, as well as of boundary-layer thickness, which are characterized by a spanwise wavelength λ. That is, the boundary layer is thickest at the upwash, where low-speed fluid is convected away from the surface, and thinnest at the downwash, where freestream fluid is swept toward the surface, as shown in Fig. 2.

The occurrence of such vortices depends on the three parameters[4]: 1) the Goertler number $G_\theta = Re_\theta(\theta/R)^{1/2}$, 2) the dimensionless wave number $\alpha\theta$, where $\alpha = 2\pi/\lambda$ is a measure of the vortex pair width or wavelength, and 3) the spatial growth parameter $\beta\theta Re_\theta$.

The critical state, where $G_\theta = G_{\theta cr}$ and $\alpha\theta = \alpha\theta_{cr}$, is the least condition for the vortices to occur and is the minimum of the neutral curve in the Goertler vortex stability diagram,[4] where G_θ is plotted against $\alpha\theta$ and θ is calculated using the Blasius boundary-layer solution. For the conditions along the neutral curve, the vortices will neither grow nor die out since $\beta = 0$. For unstable conditions on the left-hand side of the neutral curve, the vortices will grow and eventually trigger boundary-layer transition. For stable conditions on the right-hand side of the neutral curve, all of the disturbances are damped, that is, no vortices can occur.

The formation of Goertler vortices can be physically explained as follows. The fluid in the outer part of boundary layer nearer to the center of curvature of the concave surface is subjected to a larger centrifugal force than the slower moving fluid nearer to the concave surface. Therefore, it has the tendency to move toward the surface, which forces the fluid adjacent to the surface to move in the spanwise direction and then radially away from the surface,

replacing it. As the expelled fluid moves nearer to the center of curvature, it experiences a larger centrifugal force, and therefore, it tends to move back toward the concave surface. This cyclic motion forms the counter-rotating Goertler vortices.

Interest in these vortices is mainly due to their effects on boundary-layer transition and heat transfer, especially in turbomachinery applications. Goertler vortices have been observed by Kemp[5] and Han and Cox,[6] for example, on the pressure (concave) surfaces of turbine blade cascades.

The spanwise variation in boundary-layer thickness due to Goertler vortices makes the boundary-layer transition process on concave surfaces very different from that on a flat plate. Liepmann[7] found that the start of transition in the boundary layers on concave surfaces of 0.76 and 6.10 m radii of curvature occurred at Reynolds number much lower than on flat or convex surfaces, and the transition Goertler number decreased from 9 at a turbulence intensity of 0.06% to 6 at 0.3%. These findings are often quoted and used as a basis of predicting transition on concave surfaces in general (see Forest,[8] for example). Winoto and Low[9,10] found that, at the start of transitions $x_{tr,s}$ on concave surfaces of 1.0 and 3.0 m radii of curvature, the Goertler numbers based on the Blasius boundary-layer solution were between 7.5 and 8.0. Myose and Blackwelder[11] found that the secondary instability characterized by sinusoidal motion that occured prior to transition were initiated at Goertler numbers of between 7.1 and 8.1.

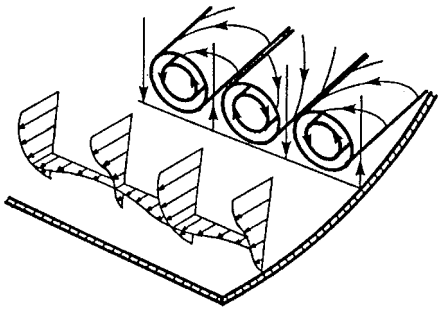

Fig. 1 Goertler vortices and the spanwise and normal distributions of streamwise velocity component.

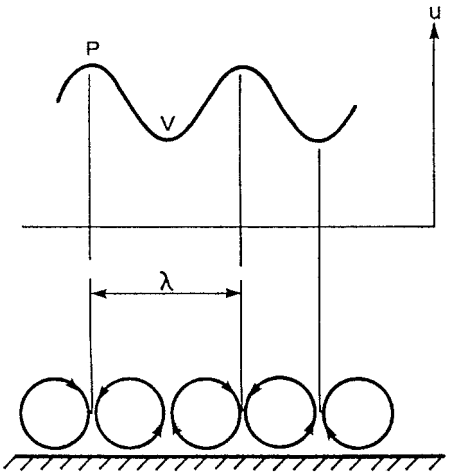

Fig. 2 Spanwise distribution of streamwise velocity component u and definitions of vortex wavelength λ, downwash P and upwash V.

An important consequence of this centrifugal instability is the possible enhancement of heat transfer in the presence of Goertler vortices. However, there have been relatively few investigations on the effect of Goertler vortices on laminar heat transfer. The earliest heat transfer measurements were by McCormack et al.,[12] in low-speed flow over a concave plate of 0.13-m radius of curvature. Their results showed a 100–150% increase in global Nusselt number on the concave plate compared with flat plate values. Martin and Brown[13] suggested that Goertler vortices, when interacting with mainstream turbulence, might account for cascade measurements of heat transfer on blade pressure surfaces greater than for a laminar boundary layer on a flat plate. Kottke[14] reported on the increase in Nusselt number up to 80%. Crane and Sabzvari[15] found enhancement of spanwise-averaged Stanton numbers for Goertler numbers greater than 10.

Crane and Leoutsakos[16] and Winoto and Low[9] confirmed that transition in such boundary-layer flows first started at the upwash regions that are viscously more unstable. Hence, there is a spanwise variation that depends on the vortex wavelength λ in the transition zone, that is, the downwash region can still be at a laminar state even though the upwash region is already transitional, as reported by Winoto and Low.[9]

In this paper, the experimental results of transition measurements obtained in boundary-layer flows along a concave surface of 2.0 m radius of curvature are presented. The aim is to study the transition region in concave surface boundary-layer flows.

II. Experimental Details

A. Experimental Setup

The experimental setup (Fig. 3) is similar to that used by Winoto and Low.[9] It consists of a perspex (plexiglass) 60-deg bend curved duct with rectangular cross section of 0.15 ×0.60 m, connected

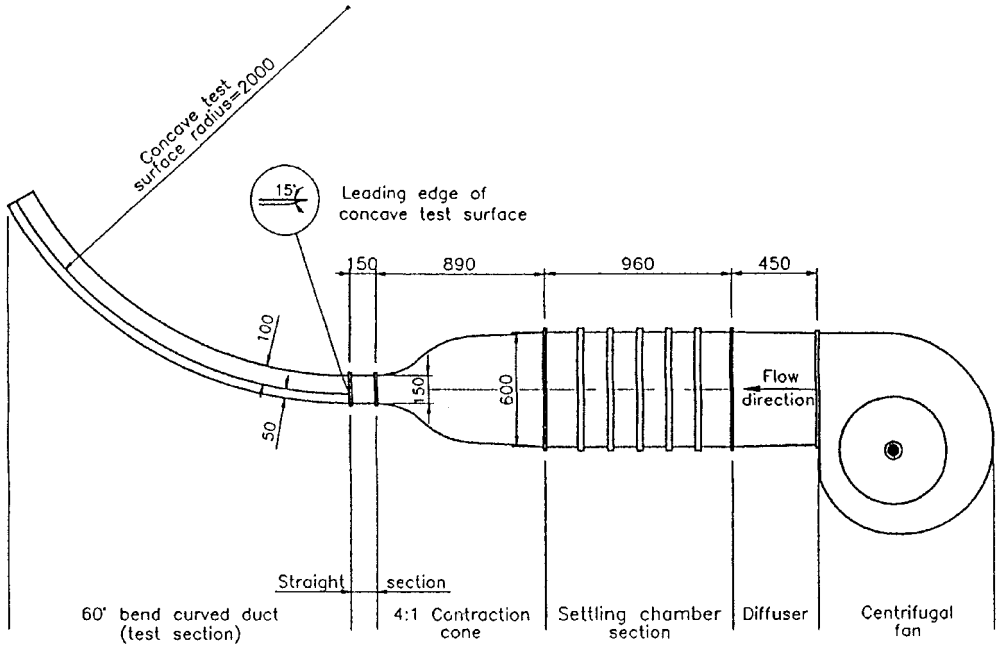

Fig. 3 Experimental setup (all dimensions in millimeters).

to a low-speed, blow-down-type wind tunnel. The wind tunnel is driven by a 0.60-m centrifugal fan powered by a 4.3-kW variable speed dc shunt-wound motor, and a small-angle diffuser connects the blower to a 0.60 ×0.60 m settling chamber. The upstream portion of the settling chamber consists of honeycomb with cells of 10 mm diameter and 50 mm length, and five removable frames, each having internal dimensions of 0.61 ×0.61 ×0.02 m^3. Fine screens of mesh 20 (per inch) and 28 standard wire gauge (0.38-mm-diam) stainless steel wire gauze are attached to the frames. A 4:1 contraction is attached downstream to the settling chamber, which reduces the flow cross-sectional area to 0.15 × 0.60 m.

The experiments were conducted on a perspex concave test surface mounted inside the curved duct at 0.05 m from the duct outer surface, forming a test section with aspect ratio of 6. The concave surface has a radius of curvature of 2.0 m and a sharp leading edge with an acute angle of 15 deg.

B. Velocity Measurement and Transition Detection

Hot-wire anemometry was used to measure the mean and fluctuating streamwise velocity components. A single sensor hot-wire probe was held by an x–y–z traversing mechanism mounted on the test section top surface and has access to the concave surface through a large opening made on the top surface. This opening is covered by a thin, curved perspex plate that can slide on the test section top surface, which makes traversing in the streamwise x, normal or radial y, and spanwise z directions possible. The streamwise distance from the leading edge and the spanwise positions were measured by means of fine markings on the test surface. A traveling microscope with reading accuracy of ±0.01 mm was used to determine the distance between the test surface and the probe. The signal from the hot-wire anemometer was first conditioned using a 200-Hz high-pass filter to remove the Tollmien–Schlichting frequency. At the same time, a low-pass filter was also used to reduce any high-frequency noise associated with the electronic circuitry. The signal was then digitized at a sampling frequency of 2 kHz using 12-bit analog to digital converter. Each sample consisted of 81.92 kB of data, which was stored in the microcomputer memory.

Because the frequency spectrum method as previously used to detect the start of transition by Winoto and Low[9,10] cannot accurately detect the end, a new intermittency method as proposed by Zhang et al.[17] was used to determine the flow transitional level in this work. In this method, when the quantity of $|\overline{u'\partial u'/\partial t}|$ over a predefined time interval (0.005 s, which equals one wavelength of the lowest frequency of the flow signals after the high-pass filter) is equal to or greater than the quantity of $C[\bar{u}(\partial u'/\partial t)_{\rm rms}/(u'\partial u'/\partial t)_{\rm rms}]$, that is,

$$\left|\overline{\frac{u'\partial u'}{\partial t}}\right| \geq C\left[\bar{u}\left(\frac{\partial u'}{\partial t}\right)_{\rm rms}\Big/\left(\frac{u'\partial u'}{\partial t}\right)_{\rm rms}\right] \tag{1}$$

the corresponding flow in the predefined time interval was regarded as turbulent, otherwise as laminar. Each flow record consists of a number of time intervals; the flow transitional level (intermittency value γ) of the record is determined by the ratio of the number of turbulent time intervals to the total number of time intervals in the record. In Eq. (1) u' and $\bar{u}$ are the fluctuating and local mean streamwise velocities, C was taken to be 2 according to the experiments, and $(\partial u'/\partial t)_{\rm rms}$ and $(u'\partial u'/\partial t)_{\rm rms}$ are both the long-time standard deviations.

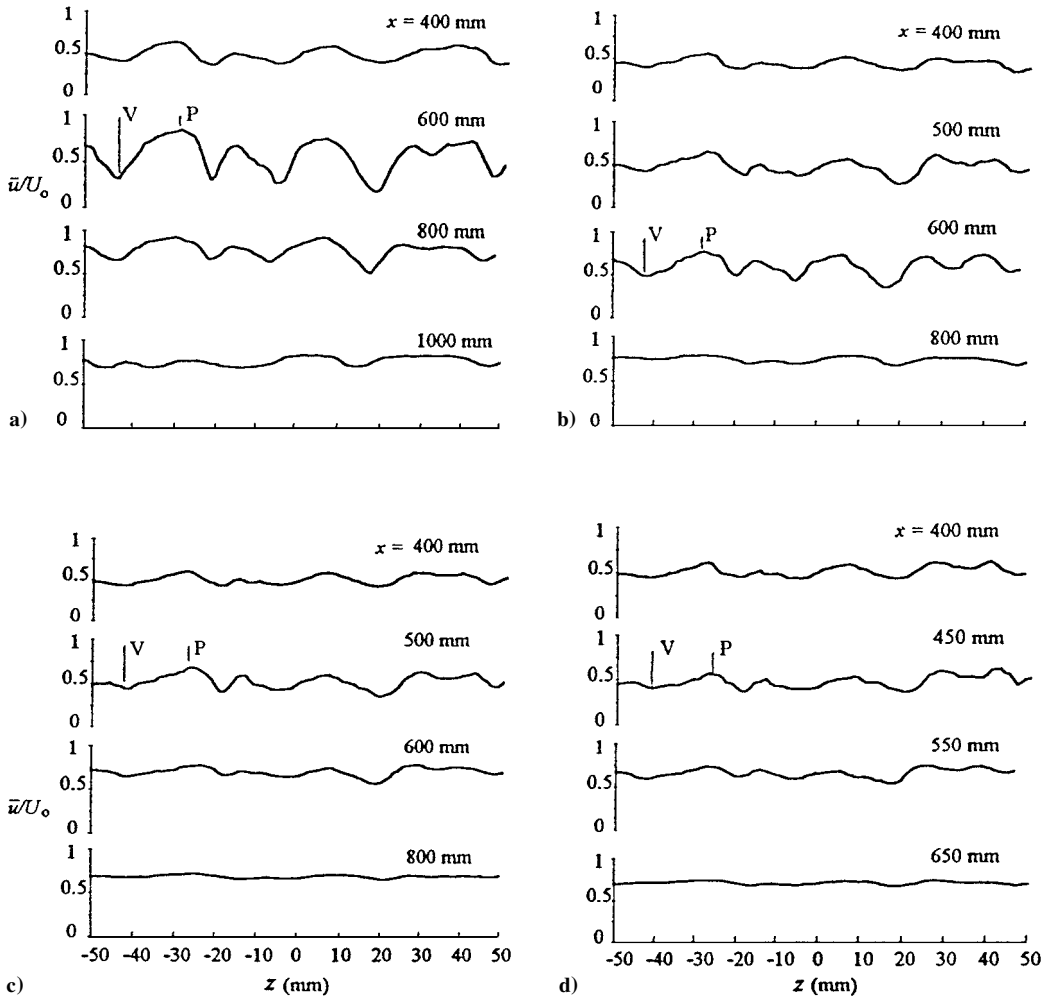

Fig. 4 Spanwise distributions of mean streamwise velocity $\bar{u}$ (normalized by freestream velocity U_0) where P and V correspond to a downwash and an upwash, respectively, at $y/\theta = 2$ for a) U_0 = 6 m/s, b) U_0 = 9 m/s, c) U_0 = 12 m/s, and d) U_0 = 15 m/s.

C. Flow Conditions and Experimental Procedure

The measurements were conducted at freestream velocity U_0 of 6.0, 9.0, 12.0, and 15.0 m/s, in which the streamwise static pressure distribution obtained from the static pressure taps along the midspan of the test section showed deviation of static pressure coefficient C_p to be less than 5%. In this freestream velocity range, the freestream turbulence intensity Tu at various streamwise positions was found to be about 0.3%.

For each freestream velocity, measurements of streamwise velocity component $\bar{u}$ were first carried out inside the boundary layer in the spanwise region defined by $z = -50$ to $+50$ mm by traversing the hot-wire probe in the spanwise direction at a normal distance y of about twice the boundary-layer momentum thickness θ (calculated using the Blasius flat-plate solution) from the test surface, at several streamwise positions. This was done to find the peaks P and valleys V in the spanwise distributions $\bar{u}$ (z) obtained, which correspond

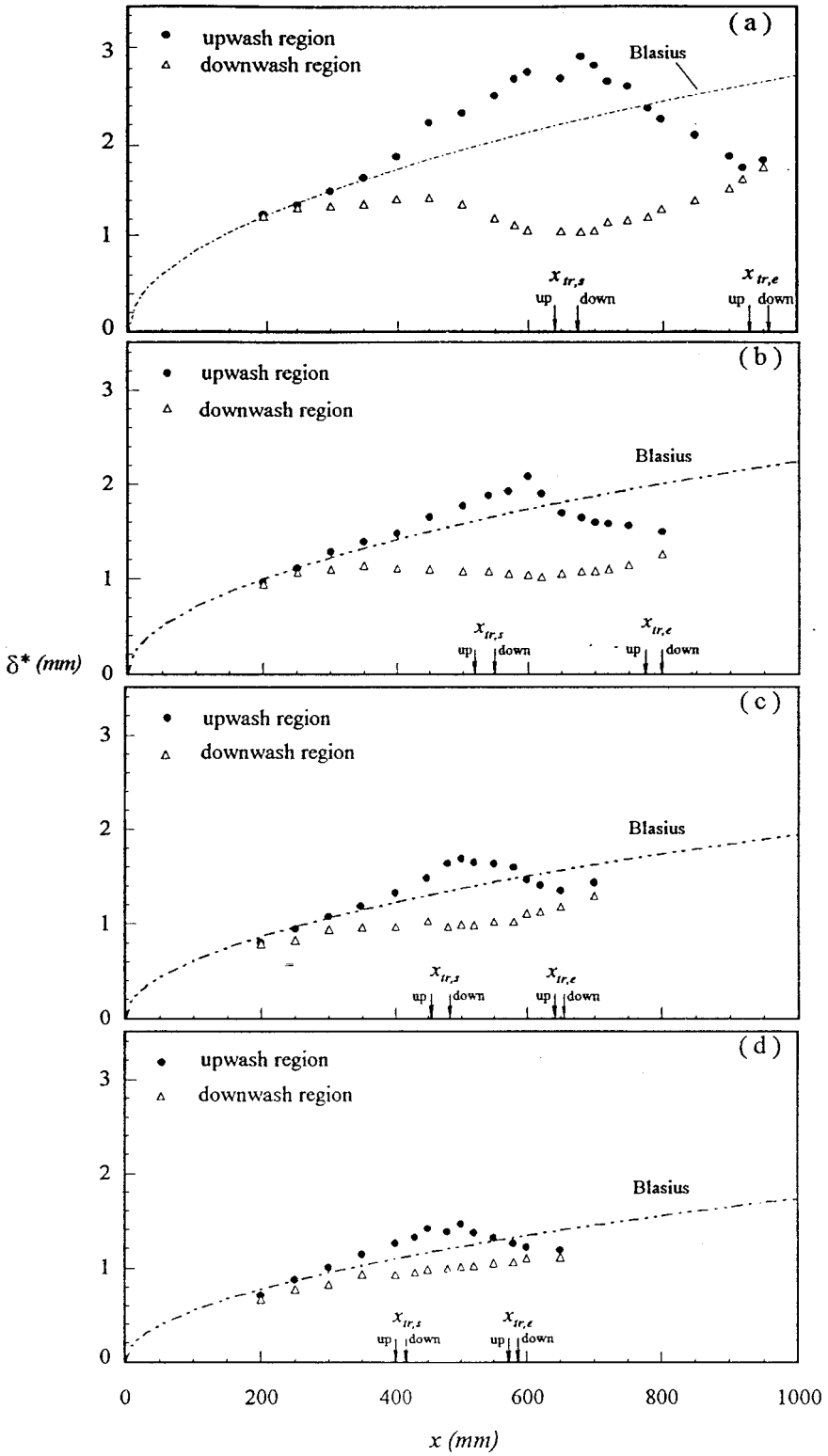

Fig. 5 Streamwise development of boundary-layer displacement thickness δ^* at upwash V and downwash P regions for a) U_0 = 6 m/s, b) U_0 = 9 m/s, c) U_0 = 12 m/s, and d) U_0 = 15 m/s.

to downwash and upwash regions, respectively, which indicate the presence of Goertler vortices (Fig. 4). Then a pair of downwash or peak P and upwash or valley V were chosen for the measurements of $\bar{u}(y)$ and $u'(y)$ at various streamwise positions. From the distributions of $\bar{u}(y)$ and $u'(y)$, the boundary-layer displacement thickness δ^* and intermittency profiles $\gamma(y)$ were obtained.

III. Results and Discussion

A. Boundary-Layer Displacement Thickness and Stability Diagram

The streamwise developments of measured boundary-layer displacement thickness δ^* at the upwash and downwash regions for $U_0 = 6.0$, 9.0, 12.0, and 15.0 m/s are presented in Fig. 5. For comparison, the corresponding Blasius boundary-layer growths are also included in the Fig. 5. The arrows indicate the transition start and end positions at the upwash and downwash regions, which are denoted by $x_{tr,s}$ (up, down) and $x_{tr,e}$ (up, down).

As shown in Fig. 5, the measured δ^* values at the upwash and downwash regions agree well with each other and with the Blasius values at the initial stages of the boundary layers (for $x \leq 250$ mm) for all U_0 values. However, with increasing x, the differences between the δ^* values at the upwash and downwash regions are increasing until some maximum values. The differences are then decreasing to zero at locations that roughly correspond to the ends of boundary-layer transition, especially for the lower freestream velocities ($U_0 = 6.0$ and 9.0 m/s). It is also observed that the differences between the δ^* at the upwash and downwash regions decrease in magnitude with increasing U_0.

To verify the stability theory, the average wavelengths of Goertler vortices obtained from the spanwise distributions of $\bar{u}$ in Figs. 4a–4d are used to compare the experimental results with those obtained by Tani,[18] Bippes,[19] Winoto and Crane,[20] Ito,[21] and Swearingen and Blackwelder[22] in the Goertler vortex stability diagram of Floryan and Saric,[23] as shown in Fig. 6. It can be seen that the present flows are well inside the unstable region of the diagram where amplification of disturbances is predicted. It is also noted that the experimental points for a particular run (that is, constant wavelength λ for a given set of conditions) generate lines of constant slope $\frac{3}{2}$. These lines can be represented by a nondimensional wavelength parameter Λ, which is defined as

$$\Lambda = (U_0 R/\nu)(\lambda/R)^{\frac{3}{2}} \tag{2}$$

For the present results, where the average wavelength $\lambda = 22.5$, 21.9, 22.1, and 22.6 mm for $U_0 = 6$, 9, 12, and 15 m/s, respectively, the corresponding wavelength parameter $\Lambda = 940$, 1350, 1820, and 2360.

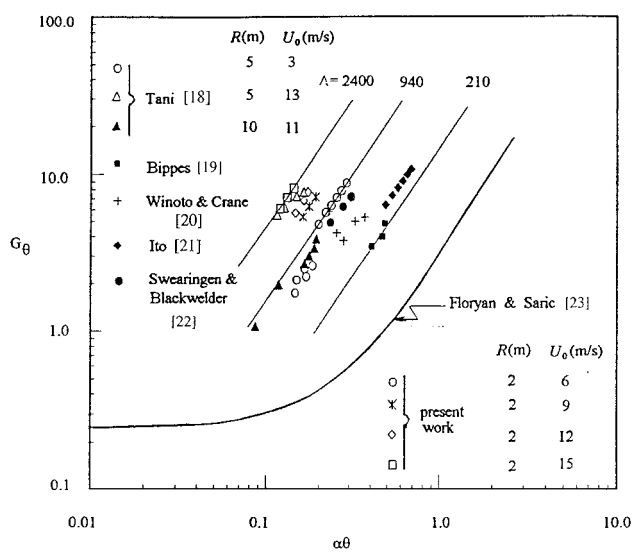

Fig. 6 Comparison of the present experimental results with some others in the Goertler vortex stability diagram of Ref. 23.

B. Turbulent Intermittency Profiles

The intermittency profiles across the boundary layer were obtained by plotting the turbulent intermittency γ vs a nondimensional boundary-layer parameter $\eta[=y/(x\nu/U_0)^{1/2}]$. For all of the freestream velocities tested, the profiles at the upwash and downwash regions at various streamwise locations are presented in Fig. 7. A nondimensional parameter $\xi = (x - x_{tr,s})/(x_{tr,e} - x_{tr,s})$ is also used to represent the streamwise location x, where $x_{tr,s}$ and $x_{tr,e}$ are, respectively, the transition-start and transition-end positions determined by γ, whose maximum value across the boundary layer first becomes nonzero at $x_{tr,s}$ and first reaches a unity at $x_{tr,e}$.

As shown in Fig. 7, for both the upwash and downwash regions, at the different free stream velocities, the intermittency profiles in different stages of transition have similar behaviors. In the earlier stages of transition (for $\gamma < 0.9$), all profiles exhibit behaviors where the intermittency increases with increasing η in the near-wall regions of the boundary layers, and then a maximum value occurs midway across the boundary layers. After reaching their maximum, γ will decrease with increasing η in the outer boundary-layer regions. In other words, for both the two spanwise regions and the different velocities, the intermittency across the boundary layers does not decreases monotonically with increasing η from the wall to the outer flows in the earlier stages of transition.

For the maximum intermittency, there are some differences between the upwash and downwash profiles. At the upwash, because the boundary layers are thicker (see Fig. 5) and there is a lower shear layer midway of the boundary layers, the intermittency profiles in these regions exhibit some fairly constant maximum values. This is more distinct for the cases of lower freestream velocities. At the downwash regions, the peak maximum intermittency values occur near the wall (for all cases at $U_0 = 6.0$ and 9.0 m/s, and higher-γ cases at $U_0 = 12.0$ and 15.0 m/s, the peak value occurs about at $\eta = 1$; for cases with low-γ value at $U_0 = 12.0$ and 15.0 m/s, it occurs about $\eta = 1.5$). This is quite similar to the values of Kuan and Wang[24] and Sohn et al.[25] for the flat-plate boundary layers and indicates that there is a strong similarity between the downwash concave surface flows and the flows on flat plates.

The maximum γ across the boundary layer in the early stages of transition does not occur near the wall, but at a distance away from the wall. This might be due to the shape of the turbulent spots in the early stages of transition. According to Cantwell et al.,[26] the shape of a turbulent spot generated near the wall has a maximum cross-sectional area away from the wall after it becomes fully developed. In the early stages of a turbulent spot evolution, there is a strong overhang in the shape of the turbulent spot. It is inferred that such an overhang results in the shape of intermittency profiles as shown in Fig. 7. The present findings in which γ is decreasing in the near-wall region of the boundary layer is also consistent with those reported by Crane et al.[16] and Walker and Solomon[27] for concave surface boundary layers. Figure 7 also shows that, at the very late stages of transition, γ is fairly constant in the near-wall region and decreases gradually in the outer region, for both the upwash and downwash regions. This implies that the turbulent spots have been fully developed at these stages.

C. Transition Start and End Positions

To identify the start of transition, the hot-wire probe was first traversed from upstream to downstream in the streamwise x direction along the upwash and downwash regions at a normal distance $y \approx 2\theta$. After a transitional signal was observed on an oscilloscope, the hot-wire probe was positioned a few millimeters before the start of transition, and data acquisition in the normal y direction was carried out to obtain turbulent intermittency profiles $\gamma(y)$ at every 5-mm interval of streamwise distance x.

Based on the intermittency profiles obtained, the streamwise positions of the starts (where the first nonzero γ values were detected in the profiles) and ends (where the first values of $\gamma = 1$ were detected in the profiles) of transition for the freestream velocities considered were determined at the upwash and downwash regions. The results are summarized in Table 1 and presented in Fig. 8, as well as indicated in Fig. 5. The maximum experimental uncertainty

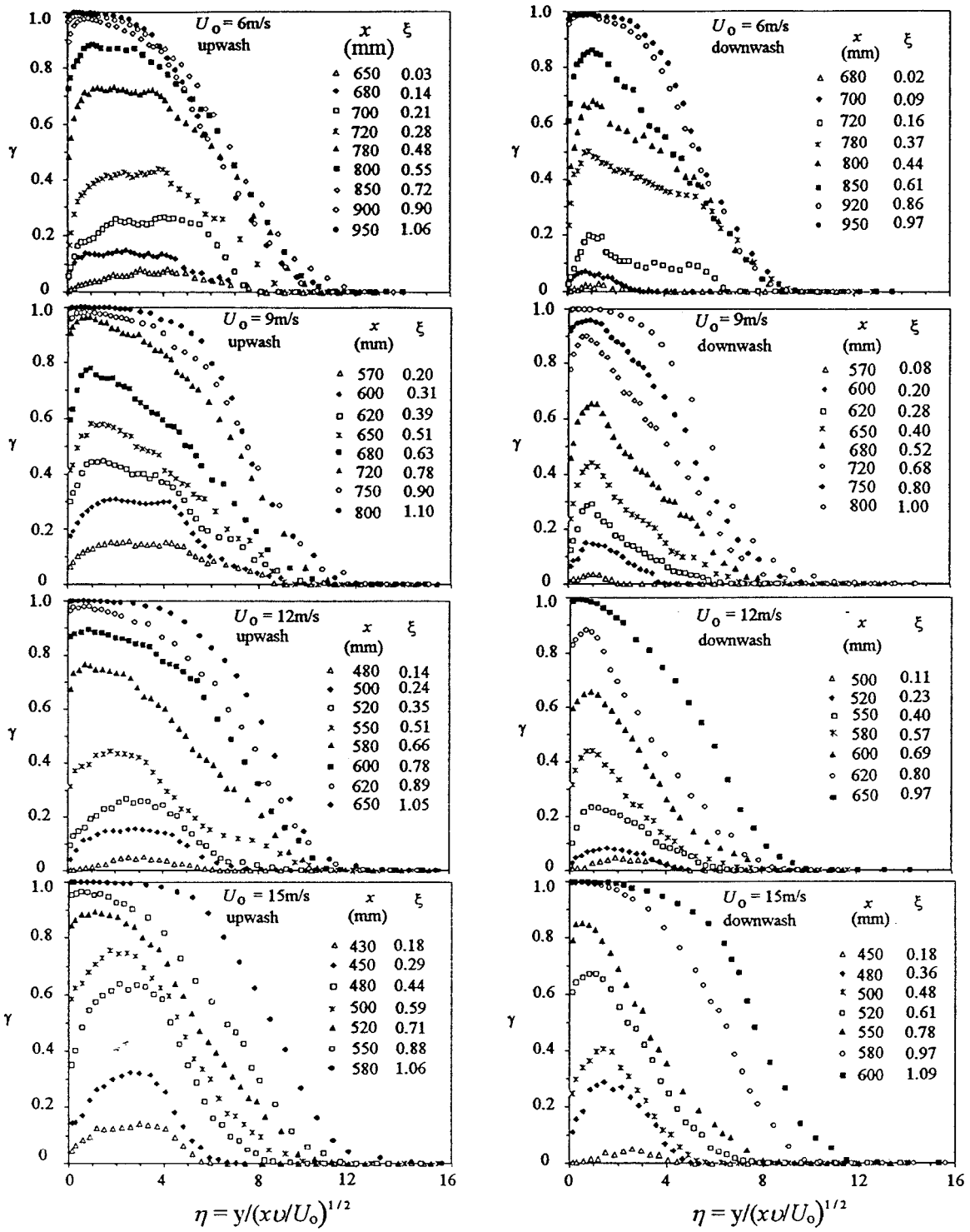

Fig. 7 Intermittency profiles at various streamwise positions at upwash V and downwash P regions for U_0 = 6, 9, 12, and 15 m/s.

estimated from repeatability tests was about ±5%. For practical reasons, the values of the boundary-layer displacement thickness and momentum thickness, respectively, $\delta^*_{tr,s}$, $\theta_{tr,s}$, and $\delta^*_{tr,e}$, $\theta_{tr,e}$, were calculated from the Blasius flat-plate boundary-layer solutions using the corresponding $x_{tr,s}$ and $x_{tr,e}$, respectively. $Re_{x,s} = x_{tr,s}U_0/\nu$, $Re_{x,e} = x_{tr,e}U_0/\nu$, $G_{\theta,s} = (U_0\theta_{tr,s}/R)^{1/2}/\nu$, and $G_{\theta,e} = U_0\theta_{tr,s}(\theta_{tr,s}/R)^{1/2}/\nu$.

Figure 8 shows the variations of the streamwise positions of transition start and end with freestream velocity U_0. Note that for all of the U_0 considered, transition starts and ends earlier at the upwash regions and later downstream at the downwash regions, as reported by Winoto and Low,[9,10] but for the start of transition only. The transition lengths ($x_{tr,e} - x_{tr,s}$) at the upwash regions are longer than those at the downwash regions. This is because at the start of transition, the three-dimensional distortions due to Goertler vortices are very strong[28] and consequently the boundary-layer flows at the upwash and downwash regions are quite different (see Fig. 5). The flows at the upwash regions are more unstable, which causes transition to occur earlier at these regions than at downwash regions. However, in the transition-endregion, as the flow becomes more turbulent, the increasing mixing gradually makes the boundary-layer homogeneous in the spanwise direction (see Figs. 1 and 5). This results in not as large a difference between the transition-end positions at the upwash and downwash regions, unlike that in the transition-start

Table 1 Parameters of boundary-layer flows on a concave surface of 2.0 m radius of curvature at transition start and end positions

Spanwise position	U_0, m/s							
	6		9		12		15	
	Upwash	Downwash	Upwash	Downwash	Upwash	Downwash	Upwash	Downwash
$x_{tr,s}$, mm	640	675	520	550	455	480	400	420
$x_{tr,e}$, mm	930	960	775	800	640	655	570	585
$x_{tr,e} - x_{tr,s}$, mm	290	285	255	250	185	175	170	165
$Re_{x,s}$, 10^5	2.51	2.65	3.06	3.24	3.57	3.77	3.92	4.12
$Re_{x,e}$, 10^5	3.56	3.77	4.56	4.71	5.02	5.14	5.59	5.69
$\delta^*_{tr,s}$, mm	2.214	2.272	1.628	1.675	1.318	1.354	1.107	1.126
$\delta^*_{tr,e}$, mm	2.666	2.709	1.987	2.020	1.564	1.538	1.320	1.332
$\theta_{tr,s}$, mm	0.848	0.871	0.624	0.642	0.506	0.519	0.424	0.430
$\theta_{tr,e}$, mm	1.022	1.039	0.762	0.774	0.600	0.609	0.504	0.511
$G_{\theta,s}$	6.85	7.13	6.49	6.77	6.31	6.57	6.06	6.28
$G_{\theta,e}$	9.07	9.29	8.75	8.96	8.15	8.29	7.90	8.00

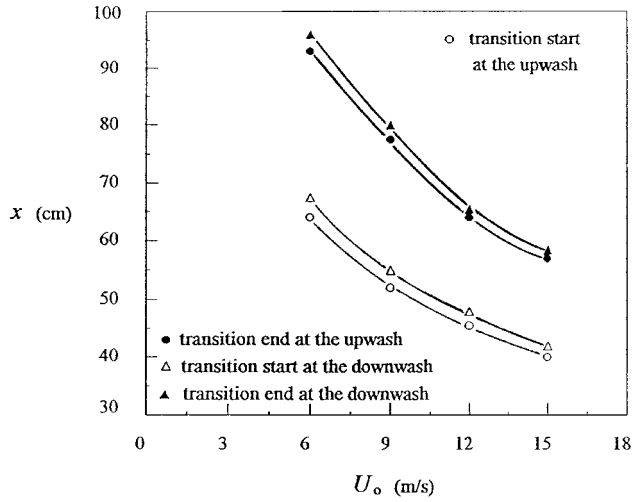

Fig. 8 Relations between transition start and end positions and freestream velocity U_0 for concave surface boundary-layer flows.

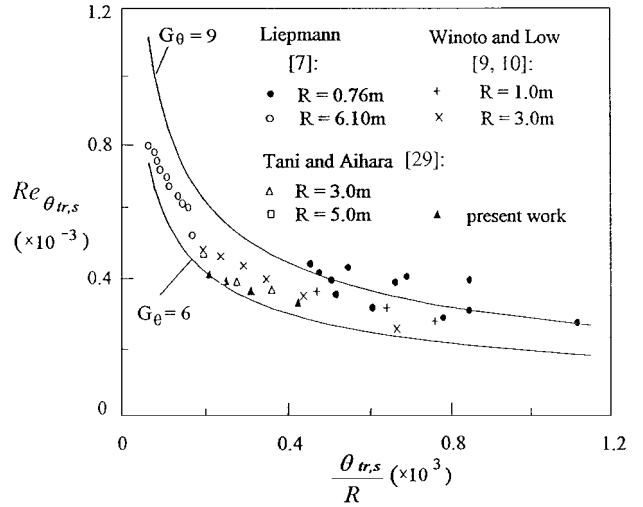

Fig. 9 Comparison of some transition experimental results for concave surface boundary-layer flows.

region. Figure 8 also shows that the transition length decreases with increasing freestream velocity, but the difference between the transition lengths at the upwash and downwash regions basically remains the same.

To compare the present results with some previous findings, the transition-start positions at the upwash regions were replotted as $Re_{\theta_{tr,s}}$ ($=U_0\theta_{tr,s}/\nu$) vs $\theta_{tr,s}$ in Fig. 9, for all of the freestream velocities. The present results lie well between the lines of $G_\theta = 6$ and 9, which are the transition criteria suggested by Liepmann,[7] like those of Tani and Aihara,[29] Winoto and Low,[9,10] and some of those of Liepmann,[7] especially for the case of $R = 6.10$ m.

IV. Conclusions

Hot-wire anemometer measurements have been made to determine the transition regions in boundary-layer flows on a concave surface of 2.0 m radius of curvature at freestream velocity $U_0 = 6.0$, 9.0, 12.0, and 15.0 m/s. Profiles of turbulent intermittency across the boundary layers at upwash and downwash regions were obtained to help determine the transition start and end at the regions.

The results show that at these two regions, the intermittency profiles obtained in different stages of transition exhibit similar behaviors for all of the freestream velocities. Intermittency value γ does not decrease with increasing y from the wall to the outer flow. Instead, a fairly constant maximum value midway across the boundary layer in the upwash region and a peak near the wall in the downwash region are, respectively, observed. The difference between the upwash and downwash intermittency profiles decreases with increasing velocity. For all of the freestream velocities considered, transition starts and ends earlier at upwash regions than at downwash regions. The transition lengths ($x_{tr,e} - x_{tr,s}$) at the upwash regions are slightly longer than those at downwash regions, but at both upwash and downwash regions they decrease with increasing freestream velocity. In terms of transition-start position at the upwash region, the present results agree well with the transition prediction $G_\theta = 6$ as suggested by Liepmann[7] at $Tu = 0.3\%$. In terms of transition-end position, $G_{\theta,e}$ ranges from 7.90 to 9.30, which can be used for a more realistic transition prediction for concave surface boundary-layer flows.

References

[1] Schlichting, H., *Boundary-Layer Theory*, 7th ed., McGraw–Hill, New York, 1979, pp. 449–488.

[2] Abu-Ghannam, B. J., and Shaw, R., "Natural Transition of Boundary Layers—The Effects of Turbulence, Pressure Gradient, and Flow History," *Journal of Mechanical Engineering Science*, Vol. 22, 1980, pp. 213–228.

[3] Goertler, H., "Instabilitat laminarer Grenzchichten an Konkaven Wanden gegenuber gewissen dreidimensionalen Storungen, ZAMM, Vol. 21, 1941, pp. 250–252 (translated as "On the Three-Dimensional Instability of Laminar Boundary Layer on Concave Walls," NACA TM 1375, 1954).

[4] Smith, A. M. O., "On the Growth of Taylor–Goertler Vortices Along Highly Concave Walls," *Quarterly of Applied, Mathematics*, Vol. 13, 1955, pp. 233–262.

[5] Kemp, A. S., "The Boundary-Layer on the Pressure Face of Turbine Blades in Cascade," Ph.D. Thesis, Cambridge Univ., Cambridge, England, U.K., 1977.

[6] Han, L. S., and Cox, W. R., "A Visual Study of Turbine Blade Pressure-Side Boundary Layers," *Journal of Engineering for Power*, Vol. 105, 1983, pp. 47–52.

[7] Liepmann, H. W., "Investigation of Boundary Layer Transition on Concave Walls," NACA Wartime Rept., ACR 4J28, 1945.

[8] Forest, A. E., "Engineering Predictions of Transitional Boundary Layers," CP-224, AGARD, 1977, pp. 22.1–22.19.

[9] Winoto, S. H., and Low, H. T., "Transition of Boundary Layer Flows in

the Presence of Goertler Vortices," *Experiments in Fluids*, Vol. 8, 1989, pp. 41–47.

[10]Winoto, S. H., and Low, H. T., "Transition of Boundary Layer Flows in the Presence of Goertler Vortices," *Experiments in Fluids*, Vol. 10, 1991, pp. 281–284.

[11]Myose, R. Y., and Blackwelder, R. F., "Controlling the Spacing of Streamwise Vortices on Concave Walls," *AIAA Journal*, Vol. 29, 1991, pp. 1901–1905.

[12]McCormack, P. D., Welker, H., and Kelleher, M., "Taylor–Goertler Vortices and Their Effect on Heat Transfer," *Journal of Heat Transfer*, Vol. 92, 1970, pp. 101–112.

[13]Martin, B. W., and Brown, A. A., "Factors Influencing Heat Transfer to the Pressure Surfaces of Gas Turbine Blades," *International Journal of Heat and Fluid Flow*, Vol. 1, 1979, pp. 107–114.

[14]Kottke, V., "Taylor–Goertler Vortices and Their Effect on Heat and Mass Transfer," *Proceedings of the 8th International Heat Transfer Conference*, Vol. 3, 1986, pp. 1139–1144.

[15]Crane, R. I., and Sabzvari, J., "Heat Transfer Visualization and Measurement in Unstable Concave-Wall Laminar Boundary Layers," American Society of Mechanical Engineers, Paper 88-GT-36, 1988.

[16]Crane, R. I., Leoutsakos, G., and Sabzvari, J., "Transition in Pressure-Surface Boundary Layers," *Journal of Turbomachinery*, Vol. 109, 1987, pp. 296–302.

[17]Zhang, D. H., Chew, Y. T., and Winoto, S. H., "A Proposed Intermittency Measurement Method for Transitional Boundary Layer Flows," *Experiments in Fluids*, Vol. 19, 1995, pp. 426–428.

[18]Tani, I., "Production of Longitudinal Vortices in the Boundary Layer Along a Curved Wall," *Journal of Geophysical Research*, Vol. 67, 1962, pp. 3075–3080.

[19]Bippes, H., "Experimentelle Untersuchung des laminar-turbulenten Umschlags an Einer Parallel Angestromten Konkave Wand," *Sitzungsberichte der Heidelberger Akademie der Wissenschaften Mathematisch-naturwissenschaftliche Klasse*, 103–108, Jahrgang 1972, 3 Abhandlung (also NASA TM-72243, March 1978).

[20]Winoto, S. H., and Crane, R. I., "Vortex Structure in Laminar Boundary Layers on a Concave Wall," *International Journal of Heat and Fluid Flow*, Vol. 2, 1980, pp. 221–231.

[21]Ito, A., "Breakdown Structure of Longitudinal Vortices Along a Concave Wall," *Journal of the Japan Society of Aeronautical and Space Science*, Vol. 33, 1985, pp. 166–173.

[22]Swearingen, J. D., and Blackwelder, R. F., "The Growth and Breakdown of Streamwise Vortices in the Presence of a Wall," *Journal of Fluid Mechanics*, Vol. 182, 1987, pp. 255–290.

[23]Floryan, J. M., and Saric, W. S., "Stability of Goertler Vortices in Boundary Layers," *AIAA Journal*, Vol. 20, 1982, pp. 316–324.

[24]Kuan, C. L., and Wang, T., "Investigation of the Intermittent Behavior of Transitional Boundary Layer Using a Conditional Averaging Technique," *Experimental Thermal and Fluid Science*, Vol. 3, 1990, pp. 157–173.

[25]Sohn, K. H., Reshotko, E., and Zaman, K. B. M. Q., "Experimental Study of Boundary Layer Transition on a Heated Flat Plate," *Boundary Layer Stability and Transition to Turbulence*, FED-Vol. 14, American Society of Mechanical Engineers, Fairfield, NJ, 1991, pp. 163–172.

[26]Cantwell, B. J., Coles, D., and Dimotakis, P. E., "Structure and Entrainment in the Plane of Symmetry of a Turbulent Spot," *Journal of Fluid Mechanics*, Vol. 89, 1978, pp. 641–672.

[27]Walker, G. J., and Solomon, W. J., "Turbulent Intermittency Measurement on an Axial Compressor Blade," *Proceedings of the 11th Australian Fluid Mechanics Conference*, 1992, pp. 1277–1280.

[28]Floryan, J. M., "On the Goertler Instability of Boundary Layers," *Progressive Aerospace Sciences*, Vol. 28, 1991, pp. 235–271.

[29]Tani, I., and Aihara, Y., "Goertler Vortices and Boundary Layer Transition," *Zeitschrift für Angewandte Mathematik und Physik*, Vol. 20, 1969, pp. 609–618.